Published in final edited form as:
J Comp Neurol. 2014 September 1; 522(13): 3075–3090. doi:10.1002/cne.23569.

Slow-pressor angiotensin II hypertension and concomitant dendritic NMDA receptor trafficking in estrogen receptor beta-containing neurons of the mouse hypothalamic paraventricular nucleus are sex and age dependent

Jose Marques-Lopes[1], **Tracey Van Kempen**[1], **Elizabeth M. Waters**[2], **Virginia M. Pickel**[1], **Costantino Iadecola**[1], and **Teresa A. Milner**[1,2]

[1]Brain and Mind Research Institute, Weill Cornell Medical College, 407 East 61st Street, New York, NY 10065, United States of America

[2]Harold and Margaret Milliken Hatch Laboratory of Neuroendocrinology, The Rockefeller University, 1230 York Avenue, New York, NY 10065, United States of America

Abstract

The incidence of hypertension increases after menopause. Similar to humans, "slow-pressor" doses of angiotensin II (AngII) increase blood pressure in young males, but not in young female mice. However, AngII increases blood pressure in aged female mice, paralleling reproductive hormonal changes. These changes could influence receptor trafficking in central cardiovascular circuits and contribute to hypertension. Increased post-synaptic NMDA receptor activity in the hypothalamic paraventricular nucleus (PVN) is crucial for the sympathoexcitation driving AngII hypertension. Estrogen receptors beta (ERβ) are present in PVN neurons. We tested the hypothesis that changes in ovarian hormones with age promote susceptibility to AngII hypertension, and influence NMDA receptor NR1 subunit trafficking in ERβ-containing PVN neurons. Transgenic mice expressing enhanced green fluorescent protein (EGFP) in ERβ-containing cells were implanted with osmotic minipumps delivering AngII (600 ng/kg/min) or saline for 2 weeks. AngII increased blood pressure in 2 month-old males and 18 month-old females, but not in 2 month-old females. By electron microscopy, NR1-silver-intensified immunogold (SIG) was mainly in ERβ-EGFP dendrites. At baseline, NR1-SIG density was greater in 2 month-old females than in 2 month-old males or 18 month-old females. After AngII infusion, NR1-SIG density was decreased in 2 month-old females, but increased in 2 month-old males and 18 month-old females. These findings suggest that, in young female mice, NR1 density is decreased in ERβ-PVN dendrites thus reducing NMDA receptor activity and preventing hypertension. Conversely, in young males and

*Address correspondence to: Drs. Jose Marques Lopes and Teresa A. Milner, Brain and Mind Research Institute, Weill Cornell Medical College, 407 East 61st Street, RM 307, New York, NY 10065, Phone: (646) 962-8274, FAX: (646) 962-0535, jod2023@med.cornell.edu, tmilner@med.cornell.edu.

CONFLICT OF INTEREST STATEMENT

The authors have no conflict of interest.

ROLE OF AUTHORS

All authors had full access to all the data in the study and take responsibility for the integrity of the data and the accuracy of the data analysis. Study concept and design: JML, EMW, CI and TAM. Preparation of tissue sections: TVK, JML. Acquisition of data: JML. Analysis and interpretation of data: JML, TAM. Drafting of the manuscript: JML, TVK, EWM, VMP, CI, TAM. Statistical analysis: JML. Obtained funding: TAM, VMP, CI. Study supervision: TAM.

aged females, NR1 density is upregulated in ERβ-PVN dendrites and ultimately leads to the neurohumoral dysfunction driving hypertension.

Keywords

hypertension; cardiovascular; estrogens; sex differences

INTRODUCTION

Hypertension is more prevalent in men than in pre-menopausal women, but this relationship is reversed following menopause (Martins et al., 2001; Wiinberg et al., 1995). In mice, administration of "slow-pressor" doses of angiotensin II (AngII) induces hypertension in 2 month-old males, but not in age-matched females (Girouard et al., 2008; Xue et al., 2013). However, AngII infusion increases blood pressure in aged female mice (Tiwari et al., 2009). This age-related induction may reflect changes in the reproductive hormonal milieu in aged mice. Whereas 2 month-old female mice experience cyclic fluctuations of ovarian hormones every 4–5 days over the course of the estrous cycle, 18 month-old female mice no longer experience regular estrous cycles (persistent estrus or diestrus) and exhibit low estrogen levels (Nelson et al., 1995). These hormonal changes could influence receptor trafficking in central cardiovascular circuits and ultimately contribute to hypertension during menopause.

Accumulating evidence has shown that estrogen plays a protective role against hypertension (Knowlton and Lee, 2012; Xue et al., 2013). Central infusion of 17β-estradiol attenuates AngII-induced hypertension in males and ovariectomized (OVX) female mice, whereas blockade of estrogen receptors (ERs) increases AngII effects in intact females (Xue et al., 2007b). However, aging, sex, and fluctuations in hormonal levels alter ERβ levels (Haywood et al., 1999; Milner et al., 2008; Mott and Pak, 2013; Zuloaga et al., 2013) and subcellular distribution in the brain, particularly in areas critically involved in neural control of blood pressure. Specifically, fluctuations in circulating estrogen levels have been shown to modulate ERα levels in the nucleus of the solitary tract (NTS) and in the paraventricular nucleus of the hypothalamus (PVN) in rats (Haywood et al., 1999; Milner et al., 2008).

The PVN plays a critical role in central cardiovascular control (Gabor and Leenen, 2012). Increased sympathoexcitatory output from the PVN is characteristic of hypertension, and NMDA receptors play a key role in regulating PVN neuronal excitability (Li et al., 2012; Li and Pan, 2010; Li et al., 2008). In spontaneously hypertensive rats (SHR), increases in basal frequency of glutamatergic excitatory postsynaptic currents and amplitude of postsynaptic NMDA currents have been shown in presympathetic PVN neurons (Li et al., 2008). Moreover, involvement of NMDA receptor activation in the PVN has been shown in AMPA and group I metabotropic glutamate receptors-induced sympathoexcitation in SHR (Li et al., 2012; Li and Pan, 2010). In the hippocampus of aged female rats, estrogens have been shown to differentially modulate subsynaptic NMDA receptor NR2 subunit density (Adams et al., 2004). Therefore, the decreasing estrogen levels observed in menopausal aged females could alter glutamatergic transmission in the PVN and blood pressure.

ERβ is expressed in spinally projecting PVN neurons that have a role in regulating sympathetic tone (Bingham et al., 2006; Laflamme et al., 1998; Milner et al., 2010). Microinjection of an ERβ agonist into the PVN of rats attenuates mineralocorticoid-induced blood pressure elevation, whereas selective knockdown of ERβ in the PVN results in blood pressure increase (Xue et al., 2013). In accordance with a protective role against hypertension, increase in neuronal nitric oxide (NO) synthase in PVN ERβ-expressing neurons has been reported in hypertensive female mice (Xue et al., 2009), and ERβ-mediated attenuation of the pressor response to PVN L-glutamate injection by administration of estrogen has been shown in male rats (Gingerich and Krukoff, 2006).

The balance between inhibitory (GABAergic) and excitatory (glutamatergic) transmission is altered in hypertension. Increased glutamatergic input and up-regulation of post-synaptic NMDA receptor activity in PVN neurons projecting to the intermediolateral (IML) cell column of the spinal cord support the enhancement of sympathetic outflow in hypertension (Gabor and Leenen, 2012; Li et al., 2008; Wang et al., 2013; Ye et al., 2012). Therefore, the present study sought to determine if differential changes occur in the density and trafficking of the obligatory NMDA receptor NR1 subunit in ERβ-expressing cells of the PVN in response to “slow-pressor” AngII infusion in an aging model of menopause. Blood pressure variation and NR1 density and subcellular distribution were compared in 2 month-old (young) females and males, and 18-month old (aged) female mice.

METHODS

Animals

General—Experimental procedures were approved by the Institutional Animal Care and Use Committees of Weill Cornell Medical College and The Rockefeller University and were in accordance with the 2011 Eighth Edition of the National Institute of Health Guide for the Care and Use of Laboratory Animals. Studies were conducted in ERβ-enhanced green fluorescent protein (ERβ–EGFP) mice on a C57BL/6 background (Milner et al., 2010). Details on the characterization of this mouse have been described previously (Milner et al., 2010). Briefly, ERβ-EGFP mice were originally developed by the GENSTAT project (www.genstat.org) at the Rockefeller University (Gong et al., 2003). Hemizygote BAC-based ERβ transgenic mice were originally on a FVB/N background and have been back-crossed with wild-type C57BL/6 mice for six generations. Two month-old males and females, and 18 month-old female mice were used. Three-four mice were housed per cage with 12:12 light/dark cycles with *ad libitum* access to food and water.

Estrous cycle determination—Estrous cycle stage was determined using vaginal smear cytology (Turner and Bagnara, 1971) daily between 9:00 and 10:00 AM. In young (pre-menopausal) mice, estrous cycles are 4–5 days long and consist of 3 primary phases: proestrus (high estrogen levels; 0.5–1 day), estrus (declining estrogen levels; 2–2.5 days) and diestrus (low estrogen and progesterone levels; 2–2.5 days). Aged (16–18 months-old, post-menopausal) mice show an acyclic, anestrous status, in which persistent estrus is observed and ovulation has ceased. Only young female mice with regular estrous cycles (at least two regular estrous cycles prior to the study beginning) were included in the study. To

control for the effects of handling, male mice were removed from their cage and handled daily.

Retrograde labeling of spinally projecting PVN neurons—Mice (n=4) were anesthetized with isofluorane (induction 5%; maintenance 1.5–2% in oxygen) and their spinal cords were exposed at the T2–T4 level through dorsal laminectomy. Using a custom-made Hamilton syringe (Model 75 SN SYR, 5 μl, 32 gauge; Reno, NV), 1 μl of 4% Fluorogold (FG, Fluorochrome Inc., Denver, CO) was pressure injected into the IML region of the spinal cord and the incision was sutured after the injection (Li et al., 2008; Wang et al., 2013).

Slow pressor AngII administration—Under isofluorane anesthesia, osmotic mini-pumps (Alzet, Durect Corporation, Cupertino, CA) containing vehicle (saline+0.1% bovin serum albumin – BSA) or AngII (600 ng · kg^{-1} · min^{-1}) were implanted subcutaneously in males (N=6 in control group, N=7 in AngII group), and in young (N=3 in both groups) and aged (N=4 in both groups) female mice. Systolic blood pressure (SBP) was measured before (baseline), and 2, 5, 9 and 13 days after mini-pump implantation in awake mice by tail-cuff plethysmography (Model MC4000; Hatteras Instruments, Cary, NC), as described previously (Coleman et al., 2010). To control for handling effects, mice were sacrificed one day after the final SBP measurements (Coleman et al., 2013; Wang et al., 2013).

Immunocytochemical procedures

Antibody characterization—For a list of the antibodies used in the present work, please see Table 1. For labeling of EGFP, a chicken polyclonal anti-GFP antibody (GFP-1020; Aves Lab Inc., San Diego, CA) was used. The GFP antibody was generated against recombinant GFP and recognizes the gene product of EGFP-expressing transgenic mice (Encinas et al., 2006). The specificity of this antibody has been demonstrated by immunohistochemistry and Western blot using transgenic mice that express GFP, resulting in one major band at ~27 kD (see data sheet for EGFP-1020 at www.aveslab.com). Moreover, absence of labeling has been shown in brain sections from mice that lack EGFP (Milner et al., 2011; Volkmann et al., 2010). Previous work from our group has shown that labeling of EGFP in ERβ-EGFP-expressing mice closely corresponds to that reported for ERβ protein and mRNA (Milner et al., 2010). The specificity of the anti-ERβ antisera used in the study of Milner et al. (2010) has been shown by double label with mRNA using in situ hybridization, preadsorption control and absence of labeling in brain sections from ERβ knock-out mice (Creutz and Kritzer, 2002; Shughrue and Merchenthaler, 2001).

To identify NR1, a monoclonal rat anti-NR1 antibody (clone 54.1; BD Biosciences, San Diego, CA) was used. Reduced labeling for this antiserum has been shown following rAAV-Cre administration into the brain of floxed NR1 mice (Beckerman and Glass, 2012; Glass et al., 2008). Specificity of the NR1 antibody was characterized via immunoprecipitation and immunohistochemistry (Brose et al., 1994; Siegel et al., 1994; Siegel et al., 1995). Western blot analysis of rat synaptic membranes and monkey hippocampal homogenates probed with the NR1 antibody resulted in one major band at ~116 kD. HEK 293 cells transfected with

cDNA encoding NR1 displayed similar results whereas non-transfected cells resulted in no bands (Siegel et al., 1994).

Detection of FG was achieved using a guinea pig antiserum against FG (Protos Biotech Corp, New York, NY). This antiserum previously showed selective staining in retrogradely labeled neurons of the mouse hippocampus (Jinno and Kosaka, 2002), rat PVN (Perello and Raingo, 2013), and rat spinal cord (Polgar et al., 2007). Immunostaining is completely blocked by preincubation with FG or Fast Blue (see data sheet for NM-101 at www.protosantibody.com).

Tissue preparation—For fluorescence immunohistochemistry, mice were deeply anesthetized with sodium pentobarbital (150 mg/kg) and their brains fixed by aortic arch perfusion sequentially with 2–3 ml saline (0.9%) containing 2% heparin followed by 30 ml of 4% paraformaldehyde (PFA) in 0.1M sodium phosphate buffer (PB; pH 7.4). After the perfusion, the brains were post-fixed for 24 h in PFA at 4°C.

For immunoelectron microscopy, mice were deeply anesthetized with sodium pentobarbital (150 mg/kg, i.p.) and fixed by aortic arch perfusion sequentially with 2–3 ml saline (0.9%) containing 2% heparin followed by 30 ml of 3.75% acrolein and 2% PFA in PB (Milner et al., 2011). After the perfusion, brains were removed and post-fixed for 30 min in 2% acrolein and 2% PFA in PB at room temperature. Brains were then cut into 5 mm coronal blocks using a brain mold (Activational Systems, Inc., Warren, MI) and sectioned (40 μm thick) on a VT1000X Vibratome (Leica Microsystems, Buffalo Grove, IL). Brain sections were stored at −20°C in cryoprotectant (30% sucrose, 30% ethylene glycol in PB) until immunocytochemical processing (Milner et al., 2011).

To ensure identical labeling conditions between experimental groups for quantitative studies (Pierce et al., 1999), two sections per animal (3 animals per group) encompassing the region of the PVN [0.70–0.94 mm caudal to bregma; Fig. 1A (Hof et al., 2000)] were marked with identifying punches, pooled into single containers and then processed through all immunocytochemical procedures together.

Dual labeling Immunofluorescence—For dual labeling of EGFP and FG, single PVN sections were removed from the cryoprotectant, rinsed thoroughly in PB and incubated in 0.5% BSA in 0.1 M TS for 30 min to minimize nonspecific binding of the antisera. Sections were then incubated in anti-GFP (1:10000) and anti-FG (1:2000) antibodies in 0.1 M Tris-buffered saline (TS, pH 7.6) with 0.1% BSA for 24 h at room temperature. The tissue was then moved to 4°C for additional 24 h. Sections were rinsed in TS and incubated sequentially in Alexa Fluor 488 goat anti-chicken IgG and Cy5 donkey anti-guinea pig IgG (both at 1:400 dilution; Invitrogen-Molecular Probes, Carlsbad, CA) for 1 hr each. Sections were mounted on gelatin-coated slides, air-dried and coverslipped with slowFade Gold reagent (Invitrogen-Molecular Probes, Grand Island, NY). Immunofluorescent photographs were acquired using a Leica (Nussloch, Germany) confocal microscope. Z-stack analysis was employed to verify dually labeled neurons.

Dual label electron microscopic immunocytochemistry—Tissue sections were processed using a pre-embedding dual immunolabeling protocol, as described previously (Milner et al., 2011). The tissue was treated with 1% sodium borohydride in 0.1 M PB for 30 min to neutralize reactive aldehydes and rinsed thoroughly in PB. The free-floating sections were then immersed in 0.5% bovine serum albumin (BSA) in 0.1 M TS for 30 min. The tissue then was incubated at room temperature in a solution of anti-NR1 (1:50) antiserum in 0.1 M TS with 0.1% BSA for 48 h. Anti-GFP (1:2500) antiserum was added to the primary antibody diluent at 24 h and the tissue was moved to 4 °C.

For immunoperoxidase detection of EGFP, sections were placed for 30 min in goat anti-chicken IgG (1:400; Jackson ImmunoResearch Inc., West Grove, PA), followed by 30 min incubation in avidin–biotin complex (Vector Laboratories, Burlingame, CA). After rinsing in TS, the bound peroxidase was visualized by reaction of the sections for 6–7 min in 3,3′-diaminobenzidine (DAB; Sigma-Aldrich Chemical Co., Milwaukee, MI) and hydrogen peroxide.

For immunogold detection of NR1, the DAB-reacted sections were rinsed, and placed overnight in a 1:50 dilution of donkey anti-mouse IgG with bound 1 nm colloidal gold [Electron Microscopy Sciences (EMS), Fort Washington, PA]. The gold particles were fixed to the tissue in 2% glutaraldehyde in 0.01M phosphate-buffered saline (PBS, pH 7.4) and rinsed in PBS followed by 0.2 M sodium citrate buffer (pH 7.4). Bound silver–gold particles were enhanced using a Silver IntenSEM kit (RPN491; GE Healthcare, Waukeska, WI) for 7 min.

Tissue sections were postfixed in 2% osmium tetroxide for 1 hr, dehydrated through a series of graded ethanols and propylene oxide, and flat-embedded in Embed-812 (EMS) between two sheets of Aclar plastic. Ultrathin sections (70 nm thickness) from the PVN were cut with a diamond knife (EMS) using a Leica EM UC6 ultratome. The sections were collected on 400-mesh thin-bar copper grids (EMS) and counterstained with uranyl acetate and lead citrate.

Ultrastructural data analyses—Sections were examined using a Tecnai transmission electron microscope. Images were collected at a magnification of 18,500. Profiles containing NR1 with EGFP immunoreactivity were classified as neuronal (soma, dendrites, axons, terminals) or glial based on criteria described by Peters et al. (1991). Dendritic profiles contained regular microtubular arrays and were usually postsynaptic to axon terminal profiles.

An equal amount of tissue from each treatment group (9596 μm2/group) was sampled for electron microscopic analysis. In each block, 50 dual-labeled dendritic profiles were photographed and analyzed. Immunoperoxidase labeling for EGFP was distinguished as an electron-dense reaction product precipitate. Silver-intensified immunogold (SIG) labeling for NR1 appeared as black electron-dense particles. To avoid false-negative labeling of smaller profiles, profiles were considered as dual-labeled if they contained electron-dense reaction product and at least one gold particle. Criteria for field selection included good morphological preservation, the presence of immunolabeling in the field, and proximity to

the plastic-tissue interface (i.e., the surface of the tissue) to avoid problems due to differences in antibody penetration (Milner et al., 2011). Tissue collection from each block was terminated when 55 pictures of dual labeled dendritic profiles were taken.

The subcellular distribution and density of NR1-SIG particles in ERβ-EGFP-labeled dendrites was determined as previously described (Coleman et al., 2013). For this, NR1-SIG particle localization was categorized as (1) plasmalemmal, (2) near plasmalemmal (particles not touching but within 70 nm from the plasma membrane), or (3) cytoplasmic. The investigator performing the quantification of SIG particles was blinded to experimental condition. Microcomputer Imaging Device software (MCID, Imaging Research Inc, Ontario, Canada) was used to determine cross-sectional diameter, perimeter, surface area, form factor, and major and minor axis lengths of each immunolabeled dendrite. Dendrites with an oblong or irregular shape (form factor value < 0.5) were excluded from the dataset. The parameters used for statistical comparisons were as follows: (1) number of plasmalemmal NR1-SIG particles on a dendrite/dendritic perimeter, (2) number of near plasmalemmal NR1-SIG particles, (3) number of cytoplasmic NR1-SIG particles/dendritic cross-sectional area, and (4) total NR1-SIG particles (sum of plasmalemmal, near plasmalemmal *and* cytoplasmic) in a dendritic profile. Dendrites were further divided in small (< 1.0 μm) and large (> 1.0 μm) based on average diameter, which correspond with distal and proximal to the cell body (Peters et al., 1991). Dendritic area and average diameter also were compared across all groups.

Statistical analysis—One-way ANOVA was used to compare SBP values or SIG particle density of three groups. Significant results were further analyzed with Tukey's HSD post hoc test. Student's t-test was used to compare two groups. Data are expressed as means ± SEM. Values were considered statistically significant when $p < 0.05$.

Figure preparation

Images were cropped in Adobe Photoshop 9.0 or PowerPoint 2010. Final adjustments to brightness, contrast, sharpness and size were done in PowerPoint 2010. These changes did not alter the original content of the raw image. Graphs were generated in Prism 5 (GraphPad Software, La Jolla, CA).

RESULTS

Distribution of ERβ-EGFP-labeled cells in the PVN

As described previously (Milner et al., 2010), low magnification showed dense packing of ERβ-EGFP-labeled cells in the PVN (Fig. 1B). When viewed at higher magnification, thick straight dendritic-like processes of ERβ-EGFP neurons could be distinguished (Fig. 1B, inset).

By electron microscopy, NR1-SIG particles were easily identifiable. NR1-SIG particles were localized in the cytoplasm, near the plasmalemma, and on the plasma membrane of ERβ-EGFP-containing dendrites (Fig. 1C). NR1-SIG particles also were observed in ERβ-EGFP-labeled terminals and somata, and in non-ERβ-containing dendrites, terminals and

glia (not shown). ERβ-EGFP-containing dendrites were contacted by numerous terminals, some of which formed asymmetric synapses.

Dual labeling with retrogradely transported tracer revealed co-localization of FG and EGFP in PVN neurons (Fig. 1F) consistent with previous studies in rats (Laflamme et al., 1998) showing that ERβ-EGFP-expressing neurons of the PVN project to the spinal cord.

Slow-pressor AngII increases SBP in males and aged females, but not in young females

Infusion of AngII significantly increased SBP in males ($p = 0.0008$) and aged females ($p = 0.0184$) on day 13 relative to their respective saline controls (Fig. 2). No significant SBP difference was observed between AngII and saline conditions in young females or in baseline SBP across all groups.

Baseline NR1 density in PVN ERβ-EGFP dendrites decreases with aging and is greater in young females than in males

Both sex and age influenced NR1-SIG density in PVN ERβ-EGFP dendrites. A significant effect of sex was observed in near plasmalemmal ($F(2, 294) = 3.675$, $p = 0.0265$) and cytoplasmic ($F(2,286) = 5.583$, $p = 0.0031$) NR1-SIG density. Post-hoc analysis revealed greater NR1-SIG density in young females than in males (near plasmalemmal: $p < 0.05$; cytoplasmic: $p < 0.01$). Near plasmalemal NR1-SIG density in dendrites of young females was greater than in aged female mice ($p = 0.0363$). Significant effects of sex and age were observed in total NR1-SIG density ($F(2,357) = 5.118$, $p = 0.0064$). Post-hoc analysis revealed greater total NR1-SIG density in young females than in males and aged females ($p < 0.05$) (Fig. 3A).

In small ERβ-EGFP dendrites (< 0.1 um in diameter), a significant effect of sex was observed in cytoplasmic NR1-SIG density ($F(2,205) = 4.908$, $p = 0.0083$) (Fig. 3C). Post-hoc analysis revealed greater cytoplasmic NR1-SIG density in young females than in males ($p < 0.01$). Greater near-plasmalemmal NR1-SIG density was observed in young females than in aged female mice ($p = 0.0400$) (Fig. 3B), and greater cytoplasmic NR1-SIG density was also seen in dendrites of aged females than in males ($p = 0.0401$) (Fig. 3C).

In large ERβ-EGFP dendrites (> 1.0 um in diameter), a significant effect of sex was observed in near plasmalemmal ($F(2, 72) = 6.284$, $p = 0.0031$) and total NR1-SIG density ($F(2, 83) = 6.470$, $p = 0.0024$). Post-hoc analysis revealed greater near plasmalemmal NR1-SIG density in young and aged females than in males (young females: $p < 0.01$; aged females $p < 0.05$) (Fig. 3B), and greater total NR1-SIG density in young females than in males ($p < 0.01$) (Fig. 3D). Age differences in females were also observed, as greater total NR1-SIG density was observed in young females than in aged female mice ($p = 0.0375$) (Fig. 3D).

No difference was found in plasmalemmal NR1-SIG density, or in diameter and area of labeled dendrites.

In ERβ-EGFP dendrites, NR1 density decreases in young females, but increases in males and aged female mice in response to AngII infusion

In males, AngII infusion increased near plasmalemmal ($p = 0.0402$) and total ($p = 0.0465$) NR1 density in large ERβ-EGFP dendrites in the PVN in comparison with saline-infused controls (Figs. 4A–B, D–E). No difference between AngII and saline infusion was found in plasmalemmal and cytoplasmic NR1-SIG density, nor in diameter and area of labeled dendrites.

In young females, AngII infusion decreased total NR1-SIG density ($p = 0.0050$) and induced a trend ($p = 0.0582$) toward a decrease in cytoplasmic NR1-SIG density in all (small+large) ERβ-EGFP dendrites in comparison with saline-infused controls (Figs. 5A–C). In small ERβ-EGFP labeled dendrites, AngII infusion decreased cytoplasmic ($p = 0.0280$, Fig. 5E) and total ($p = 0.0235$, Fig. 5F) NR1-SIG density. In large ERβ-EGFP labeled dendrites, AngII infusion decreased near plasmalemmal ($p = 0.05$, Fig. 5D) and total ($p = 0.0043$, Fig. 5F) NR1-SIG density. No difference between AngII and saline infusion was found in plasmalemmal NR1-SIG density, nor in diameter and area of labeled dendrites.

In aged females, AngII infusion increased near plasmalemmal ($p = 0.05$) and total ($p = 0.0086$) NR1-SIG density in all ERβ-EGFP-labeled dendrites (Figs. 6A–B, C). In small dendrites, AngII infusion increased near plasmalemmal ($p = 0.0011$, Fig. 6D) and total ($p = 0.0076$, Fig. 6E) NR1-SIG density. No difference between AngII and saline infusion was found in plasmalemmal and cytoplasmic NR1-SIG density, nor in diameter and area of labeled dendrites.

DISCUSSION

This study demonstrates sex differences in NR1 subunit density and trafficking in ERβ-EGFP dendrites in the mouse PVN. Age differences in females are also shown. We found that at baseline young females had greater NR1 density in ERβ-EGFP PVN dendrites than both males and aged females. This difference from the other two groups persisted in young female mice following sub-pressor infusion of AngII. Relative to saline controls, near plasmalemmal, cytoplasmic, and total NR1 density was lower in young females receiving AngII with no increase in SBP (Fig. 7). Yet, near plasmalemmal and total NR1 densities were increased in males and aged females, and both groups demonstrated an AngII-induced increase in SBP (Fig. 7). These findings suggest a robust estrogen-dependent post-synaptic NMDA receptor trafficking in ERβ-containing PVN neurons, which could increase glutamatergic activity and play a role in the increased susceptibility to hypertension in menopause.

Methodological considerations

Tail-cuff plethysmography is a reliable non-invasive method to compare SBP measurements between groups (Capone et al., 2010; Capone et al., 2012; Coleman et al., 2013; Wang et al., 2013). However, the use of tail-cuff plethysmography to measure SBP in mice may induce restraint and thermal stress (Gross and Luft, 2003; Mattson, 1998). As the amount of neural outflow to the cardiovascular system is influenced by restraint stress (Krukoff, 1998), we

cannot rule out that stress could be a confounding factor in the blood pressure increases of the present study. Furthermore, estrogen modulates cardiovascular responses to stress. Previous work has shown that estrogen administration attenuates increases in blood pressure, heart rate, and number of activated neurons induced by restraint stress in OVX rats (Cherney et al., 2003; Morimoto et al., 2004; Ueyama et al., 2006). To minimize stress, the animals were handled by the same experimenter and at the same time of day throughout the study. Moreover, the brains were harvested one-day after the final blood pressure measurement.

Estrous cycle determination was done in all female mice to ensure that young females had regular pre-menopause estrous cycles of 4–5-days with proestrus, estrus and diestrus stages, and that aged females were “post-menopausal”, showing an acyclic, anestrous status. Previous studies by our group and others found differences in ERβ mRNA and protein levels in the rodent hippocampus comparing proestrus with estrus and diestrus (Mitterling et al., 2010; Szymczak et al., 2006). Therefore, female mice that were at proestrus (high estrogen levels) on the day of perfusion were not included in the ultrastructural studies. No day-to-day effects of estrous cycle fluctuations on SBP measurements were found in young female mice.

The present study utilized the pre-embedding immunogold-silver technique to localize antisera selectively recognizing NR1. Although SIG labeling can yield lower estimates of receptor number than immunoperoxidase labeling due to limited reagent penetration (Leranth and Pickel, 1989), this limitation did not likely affect comparisons between groups since (a) PVN sections were pooled and processed together to control for differences in antibody penetration (Pierce et al., 1999), and (b) ultrathin sections were collected from the tissue-plastic interface where immunoreagent access is maximal (Milner et al., 2011). For each mouse, a similar number of dual labeled dendrites were collected to insure that between-group comparisons were not affected by pre-embedding SIG limitations. By controlling these factors, variability between animals in each experimental group was minimal. Analysis of NR1-SIG density in non-ERβ-containing dendrites was not performed, as these dendrites arise from a mixed population of neurons.

Labeling of EGFP and NR1 in the PVN

Labeling of ERβ-EGFP-expressing PVN neurons with retrogradely transported tracer from the spinal cord is in accordance with previous studies (Bingham et al., 2006; Laflamme et al., 1998; Milner et al., 2010). Involvement of PVN spinally projecting neurons in cardiovascular regulation has been shown (Badoer, 2001; Bains and Ferguson, 1995; Nunn et al., 2011). Moreover, PVN neurons may further regulate sympathetic nerve activity via projections (direct or collaterals of PVN-IML connections) to the rostral ventrolateral medulla (RVLM), another key area in the regulation of sympathetic outflow (Badoer, 2001).

As previously described (Milner et al., 2010), immunoperoxidase reaction product for EGFP in the PVN filled somata and dendrites. NR1-SIG particles were discretely localized within neuronal profiles and easily quantifiable. These features facilitated between group comparisons at the electron microscopic level. NR1-SIG immunoreactivity was found in the cytoplasm, near the plasmalemma and, to a lesser extent, on the plasmalemma of dendrites,

terminals and somata in the PVN. NMDA receptors are transported to the plasma membrane after subunit assembly in the endoplasmic reticulum and processing in the Golgi apparatus (Wenthold et al., 2003). The extrasynaptic population of NMDA receptors has been suggested to represent receptors that are awaiting incorporation into the synapse (Wenthold et al., 2003). Furthermore, activity-dependent endocytosis of NMDA receptors may preferentially occur at an extrasynaptic site (Nong et al., 2003; Wenthold et al., 2003). Therefore, near plasmalemmal NR1 may represent functional NMDA receptors being trafficked to/from the plasmalemma.

Sex and age differences in susceptibility to slow pressor AngII-elicited hypertension

Our results confirm and extend previous studies (Girouard et al., 2008; Xue et al., 2007a; 2013; Xue et al., 2005) showing that slow-pressor infusion of AngII elicited blood pressure increase in males, but not in young females, while aged female mice were also susceptible to hypertension. Both the sex difference in young animals and the age difference in females at reproductive stage characterized by low estrogen levels point to a role for estrogen in preventing hypertension development. Previous work has shown that central infusion of 17β-estradiol attenuates AngII-induced hypertension in males and OVX females, whereas in intact females, normally unresponsive to AngII effects, blockade of ER results in an increase in blood pressure (Xue et al., 2007b). Moreover, 17β-estradiol has been shown to inhibit AngII-induced increases in sympathetic outflow in male mice (Xue et al., 2008). Young males, but not age-matched females demonstrate blunted bradycardic responses to AngII infusion (Xue et al., 2005). In the blood-brain barrier-deprived subfornical organ, which sends excitatory projections to the PVN (Ferguson, 2009; Lind et al., 1982; Miselis, 1981), estrogen may further inhibit central AngII effects by reducing AngII binding to angiotensin type 1 (AT1) receptors (Kisley et al., 1999). Therefore, the greater estrogen levels observed in young “pre-menopausal” females may confer protection to AngII-induced blood pressure increases. Moreover, aging and sex are both known to alter central ERβ expression levels (Mott and Pak, 2013; Zuloaga et al., 2013), which may also explain the greater susceptibility to AngII-elicited SBP increases in males and aged females observed in our study.

Sex and age differences in baseline NR1 density in PVN ERβ-EGFP dendrites

Young female mice showed greater baseline NR1 density in PVN ERβ-EGFP dendrites than males and aged females. Small (< 1.0 μm in average diameter) and large (> 1.0 μm) dendrites correspond to distal and proximal dendrites, respectively. Therefore, in distal ERβ-EGFP PVN dendrites, young and aged females show a larger cytoplasmic pool of NR1 than males, and young females show greater near-plasmalemmal NR1 density than aged females. Conversely, in proximal ERβ-EGFP PVN dendrites, young females show greater total NR1 density than males and aged female mice, whereas young and aged females show greater near-plasmalemmal NR1 density than males. Previous studies in hippocampal CA1 pyramidal neurons have shown distance-dependent functional differences in expression of synaptic strength in dendrites. Whereas the synaptic strength at proximal dendrites depends on the ability to depolarize the soma/axon, distal dendrites influence neuronal activity through large local depolarizations and heterosynaptic potentiation of proximal synapses – expressed by increased AMPA and NMDA receptor activity (Han and Heinemann, 2013; Nicholson et al., 2006; Remondes and Schuman, 2002). Previous work in other brain regions

has shown changes in baseline expression of NMDA receptor subunits with aging. In the hippocampus, NR1 mRNA levels have been shown to decrease in males, but increase in female rats with aging (Adams et al., 2001a; Adams et al., 2001b; Magnusson, 2000). Also, NR1 mRNA levels negatively correlate with amount of time elapsed after OVX (Adams et al., 2001b). In agreement with the present findings, Zuo et al. (1996) showed a reduction in NR1 mRNA expression in the preoptic area and arcuate nucleus of the hypothalamus in middle-aged females in comparison with young females rats. Moreover, NR1 mRNA levels in the hypothalamic medial eminence were increased in intact rats, but decreased in OVX rats with aging (Gore, 2001), suggesting a role of ovarian factors other than estrogen in the regulation of NR1 expression. Altogether, these differences in NR1 mRNA and protein levels could influence short-term excitability and long-term gene expression.

Both sex and age influence NR1 density in PVN ERβ-EGFP dendrites in response *to AngII infusion*

The observed effect of slow-pressor AngII infusion on NR1 density in dendrites of ERβ-EGFP neurons in the PVN of in young females is opposite to that seen males and aged female mice. Whereas an overall decrease in NR1 density is observed in young females following AngII infusion, near plasmalemmal and total NR1 density increase in males and aged females in proximal and distal dendrites, respectively. Additional studies using aged male mice are needed to evaluate if aging explains this difference. Involvement of NMDA receptors of the PVN in the increased sympathoexcitation in hypertension is well established (Cui et al., 2013; Li and Pan, 2007; Li et al., 2008; Zheng et al., 2011). Increased pre- and post-synaptic NMDA receptor function in the PVN has been demonstrated in SHR (Li et al., 2008). Using the same hypertension model as the present study, work from our group has shown AngII-induced increases in post-synaptic NMDA receptor activity in spinally projecting neurons of the PVN, both at baseline and after local application of NMDA (Wang et al., 2013).

Near plasmalemmal accumulation of NR1 may result from desensitization/internalization of NMDA receptors that occurs in response to repetitive activation (Nakamichi and Yoneda, 2005). In association with the increased near plasmalemmal NR1 density, the observation that cytoplasmic NR1 density was unchanged and total NR1 density was increased by AngII suggests enhanced synthesis and/or decreased degradation of NR1. This also suggests that internalized NR1 may be recycled to the plasma membrane instead of being degraded. Regarding the increased total NR1 density, previous studies showed up-regulation of NR1 mRNA expression and protein levels in the PVN of rats with a coronary ligation model of chronic heart failure (Li et al., 2003; Zheng et al., 2011). Moreover, increased AMPA receptor GluR1 subunit density in SHR and deoxycorticosterone acetate-salt rats has been shown in the NTS (Aicher et al., 2003; Hermes et al., 2008). Taken together, the present results suggest that decreased degradation and/or up-regulation of total NR1 expression and increased near plasmalemmal density in ERβ-EGFP dendrites in the PVN may contribute to the increased glutamatergic transmission and resulting sympathoexcitation observed in “slow-pressor” AngII hypertension.

In young female mice, AngII infusion decreased near plasmalemmal, cytoplasmic and total NR1 density in ERβ-EGFP dendrites in the PVN. Decreased NR1 synthesis or degradation of internalized NR1 subunits rather than return to the plasmalemma could explain the overall decrease in NR1 density and expression after 14 d of AngII infusion. In line with the present results, Gingerich and Krukoff (2006) showed that estrogen attenuates L-glutamate-induced pressor response in the PVN of male rats, an effect mediated by ERβ, NO production and GABA-A receptors. Likewise, increased NO production in ER-containing neurons of the PVN after AngII infusion has been shown in female mice (Xue et al., 2009). Moreover, Xue et al. (2013) showed that silencing ERβ in the PVN of OVX rats augmented aldosterone-induced hypertension and reactive oxygen species production. Thus, the present results suggest the existence of an additional adaptation mechanism in ERβ-expressing neurons of the PVN, in that increased degradation or decreased synthesis of NMDA receptors would dampen glutamate transmission following AngII-infusion in young female mice. A comparable adaptation would not occur in males and aged females, suggesting a protective role of estrogen mediated by ERβ in the PVN.

In conclusion, our results show sex differences in baseline NR1 density and in changes in NR1 density in response to AngII infusion in ERβ-containing dendrites of the PVN. Age differences in females are also observed. These effects are associated with differential effects of AngII in blood pressure. Therefore, our results support the increasing body of evidence showing a central protective role of estrogen on the development of hypertension, and neurobiological changes in cardiovascular control associated with the increased incidence of hypertension in menopause. Future work will disentangle the effects of menopause from the role of aging, and evaluate changes in PVN post-synaptic NMDA receptor trafficking and density in peri-menopause.

Acknowledgments

GRANT SUPPORT: NIH grants HL098351, DA08259 & AG016765 (TAM), HL096571 (CI, VMP, TAM), and AG059850 (EMW), T32 DA007274 (TAV)

We would like to thank Andreina Gonzalez, Eugene Ogorodnik and Jolanta Gorecka for their excellent technical assistance.

LITERATURE CITED

Adams MM, Fink SE, Janssen WG, Shah RA, Morrison JH. Estrogen modulates synaptic N-methyl-D-aspartate receptor subunit distribution in the aged hippocampus. The Journal of comparative neurology. 2004; 474(3):419–426. [PubMed: 15174084]

Adams MM, Morrison JH, Gore AC. N-methyl-D-aspartate receptor mRNA levels change during reproductive senescence in the hippocampus of female rats. Exp Neurol. 2001a; 170(1):171–179. [PubMed: 11421594]

Adams MM, Oung T, Morrison JH, Gore AC. Length of postovariectomy interval and age, but not estrogen replacement, regulate N-methyl-D-aspartate receptor mRNA levels in the hippocampus of female rats. Exp Neurol. 2001b; 170(2):345–356. [PubMed: 11476600]

Aicher SA, Sharma S, Mitchell JL. Structural changes in AMPA-receptive neurons in the nucleus of the solitary tract of spontaneously hypertensive rats. Hypertension. 2003; 41(6):1246–1252. [PubMed: 12695422]

Badoer E. Hypothalamic paraventricular nucleus and cardiovascular regulation. Clinical and experimental pharmacology & physiology. 2001; 28(1–2):95–99. [PubMed: 11153547]

Bains JS, Ferguson AV. Paraventricular nucleus neurons projecting to the spinal cord receive excitatory input from the subfornical organ. The American journal of physiology. 1995; 268(3 Pt 2):R625–633. [PubMed: 7900904]

Beckerman MA, Glass MJ. The NMDA-NR1 receptor subunit and the mu-opioid receptor are expressed in somatodendritic compartments of central nucleus of the amygdala neurons projecting to the bed nucleus of the stria terminalis. Exp Neurol. 2012; 234(1):112–126. [PubMed: 22227057]

Bingham B, Williamson M, Viau V. Androgen and estrogen receptor-beta distribution within spinal-projecting and neurosecretory neurons in the paraventricular nucleus of the male rat. The Journal of comparative neurology. 2006; 499(6):911–923. [PubMed: 17072840]

Brose N, Huntley GW, Stern-Bach Y, Sharma G, Morrison JH, Heinemann SF. Differential assembly of coexpressed glutamate receptor subunits in neurons of rat cerebral cortex. The Journal of biological chemistry. 1994; 269(24):16780–16784. [PubMed: 8207001]

Capone C, Faraco G, Anrather J, Zhou P, Iadecola C. Cyclooxygenase 1-derived prostaglandin E2 and EP1 receptors are required for the cerebrovascular dysfunction induced by angiotensin II. Hypertension. 2010; 55(4):911–917. [PubMed: 20194308]

Capone C, Faraco G, Peterson JR, Coleman C, Anrather J, Milner TA, Pickel VM, Davisson RL, Iadecola C. Central cardiovascular circuits contribute to the neurovascular dysfunction in angiotensin II hypertension. The Journal of neuroscience : the official journal of the Society for Neuroscience. 2012; 32(14):4878–4886. [PubMed: 22492044]

Cherney A, Edgell H, Krukoff TL. NO mediates effects of estrogen on central regulation of blood pressure in restrained, ovariectomized rats. American journal of physiology Regulatory, integrative and comparative physiology. 2003; 285(4):R842–849.

Coleman CG, Wang G, Faraco G, Marques Lopes J, Waters EM, Milner TA, Iadecola C, Pickel VM. Membrane trafficking of NADPH oxidase p47(phox) in paraventricular hypothalamic neurons parallels local free radical production in angiotensin II slow-pressor hypertension. J Neurosci. 2013; 33(10):4308–4316. [PubMed: 23467347]

Coleman CG, Wang G, Park L, Anrather J, Delagrammatikas GJ, Chan J, Zhou J, Iadecola C, Pickel VM. Chronic intermittent hypoxia induces NMDA receptor-dependent plasticity and suppresses nitric oxide signaling in the mouse hypothalamic paraventricular nucleus. J Neurosci. 2010; 30(36):12103–12112. [PubMed: 20826673]

Creutz LM, Kritzer MF. Estrogen receptor-beta immunoreactivity in the midbrain of adult rats: regional, subregional, and cellular localization in the A10, A9, and A8 dopamine cell groups. The Journal of comparative neurology. 2002; 446(3):288–300. [PubMed: 11932944]

Cui BP, Li P, Sun HJ, Ding L, Zhou YB, Wang JJ, Kang YM, Zhu GQ. Ionotropic glutamate receptors in paraventricular nucleus mediate adipose afferent reflex and regulate sympathetic outflow in rats. Acta physiologica. 2013

Encinas JM, Vaahtokari A, Enikolopov G. Fluoxetine targets early progenitor cells in the adult brain. Proceedings of the National Academy of Sciences of the United States of America. 2006; 103(21): 8233–8238. [PubMed: 16702546]

Ferguson AV. Angiotensinergic regulation of autonomic and neuroendocrine outputs: critical roles for the subfornical organ and paraventricular nucleus. Neuroendocrinology. 2009; 89(4):370–376. [PubMed: 19342823]

Gabor A, Leenen FH. Central neuromodulatory pathways regulating sympathetic activity in hypertension. Journal of applied physiology. 2012; 113(8):1294–1303. [PubMed: 22773773]

Gingerich S, Krukoff TL. Estrogen in the paraventricular nucleus attenuates L-glutamate-induced increases in mean arterial pressure through estrogen receptor beta and NO. Hypertension. 2006; 48(6):1130–1136. [PubMed: 17075034]

Girouard H, Lessard A, Capone C, Milner TA, Iadecola C. The neurovascular dysfunction induced by angiotensin II in the mouse neocortex is sexually dimorphic. American journal of physiology Heart and circulatory physiology. 2008; 294(1):H156–163. [PubMed: 17982007]

Glass MJ, Hegarty DM, Oselkin M, Quimson L, South SM, Xu Q, Pickel VM, Inturrisi CE. Conditional deletion of the NMDA-NR1 receptor subunit gene in the central nucleus of the amygdala inhibits naloxone-induced conditioned place aversion in morphine-dependent mice. Exp Neurol. 2008; 213(1):57–70. [PubMed: 18614169]

Gong S, Zheng C, Doughty ML, Losos K, Didkovsky N, Schambra UB, Nowak NJ, Joyner A, Leblanc G, Hatten ME, Heintz N. A gene expression atlas of the central nervous system based on bacterial artificial chromosomes. Nature. 2003; 425(6961):917–925. [PubMed: 14586460]

Gore AC. Gonadotropin-releasing hormone neurons, NMDA receptors, and their regulation by steroid hormones across the reproductive life cycle. Brain research Brain research reviews. 2001; 37(1–3): 235–248. [PubMed: 11744089]

Gross V, Luft FC. Exercising restraint in measuring blood pressure in conscious mice. Hypertension. 2003; 41(4):879–881. [PubMed: 12623867]

Han EB, Heinemann SF. Distal dendritic inputs control neuronal activity by heterosynaptic potentiation of proximal inputs. J Neurosci. 2013; 33(4):1314–1325. [PubMed: 23345207]

Haywood SA, Simonian SX, van der Beek EM, Bicknell RJ, Herbison AE. Fluctuating estrogen and progesterone receptor expression in brainstem norepinephrine neurons through the rat estrous cycle. Endocrinology. 1999; 140(7):3255–3263. [PubMed: 10385422]

Hermes SM, Mitchell JL, Silverman MB, Lynch PJ, McKee BL, Bailey TW, Andresen MC, Aicher SA. Sustained hypertension increases the density of AMPA receptor subunit, GluR1, in baroreceptive regions of the nucleus tractus solitarii of the rat. Brain research. 2008; 1187:125–136. [PubMed: 18031714]

Jinno S, Kosaka T. Immunocytochemical characterization of hippocamposeptal projecting GABAergic nonprincipal neurons in the mouse brain: a retrograde labeling study. Brain research. 2002; 945(2): 219–231. [PubMed: 12126884]

Knowlton AA, Lee AR. Estrogen and the cardiovascular system. Pharmacology & therapeutics. 2012; 135(1):54–70. [PubMed: 22484805]

Krukoff TL. Central regulation of autonomic function: no brakes? Clinical and experimental pharmacology & physiology. 1998; 25(6):474–478. [PubMed: 9673828]

Laflamme N, Nappi RE, Drolet G, Labrie C, Rivest S. Expression and neuropeptidergic characterization of estrogen receptors (ERalpha and ERbeta) throughout the rat brain: anatomical evidence of distinct roles of each subtype. Journal of neurobiology. 1998; 36(3):357–378. [PubMed: 9733072]

Li DP, Byan HS, Pan HL. Switch to glutamate receptor 2-lacking AMPA receptors increases neuronal excitability in hypothalamus and sympathetic drive in hypertension. J Neurosci. 2012; 32(1):372–380. [PubMed: 22219297]

Li DP, Pan HL. Glutamatergic inputs in the hypothalamic paraventricular nucleus maintain sympathetic vasomotor tone in hypertension. Hypertension. 2007; 49(4):916–925. [PubMed: 17309953]

Li DP, Pan HL. Increased group I metabotropic glutamate receptor activity in paraventricular nucleus supports elevated sympathetic vasomotor tone in hypertension. American journal of physiology Regulatory, integrative and comparative physiology. 2010; 299(2):R552–561.

Li DP, Yang Q, Pan HM, Pan HL. Pre- and postsynaptic plasticity underlying augmented glutamatergic inputs to hypothalamic presympathetic neurons in spontaneously hypertensive rats. The Journal of physiology. 2008; 586(6):1637–1647. [PubMed: 18238817]

Li YF, Cornish KG, Patel KP. Alteration of NMDA NR1 receptors within the paraventricular nucleus of hypothalamus in rats with heart failure. Circulation research. 2003; 93(10):990–997. [PubMed: 14576197]

Lind RW, Van Hoesen GW, Johnson AK. An HRP study of the connections of the subfornical organ of the rat. The Journal of comparative neurology. 1982; 210(3):265–277. [PubMed: 7142442]

Magnusson KR. Declines in mRNA expression of different subunits may account for differential effects of aging on agonist and antagonist binding to the NMDA receptor. J Neurosci. 2000; 20(5): 1666–1674. [PubMed: 10684868]

Martins D, Nelson K, Pan D, Tareen N, Norris K. The effect of gender on age-related blood pressure changes and the prevalence of isolated systolic hypertension among older adults: data from NHANES III. The journal of gender-specific medicine : JGSM : the official journal of the Partnership for Women's Health at Columbia. 2001; 4(3):10–13. 20.

Mattson DL. Long-term measurement of arterial blood pressure in conscious mice. The American journal of physiology. 1998; 274(2 Pt 2):R564–570. [PubMed: 9486319]

Milner TA, Drake CT, Lessard A, Waters EM, Torres-Reveron A, Graustein B, Mitterling K, Frys K, Iadecola C. Angiotensin II-induced hypertension differentially affects estrogen and progestin receptors in central autonomic regulatory areas of female rats. Exp Neurol. 2008; 212(2):393–406. [PubMed: 18533148]

Milner TA, Thompson LI, Wang G, Kievits JA, Martin E, Zhou P, McEwen BS, Pfaff DW, Waters EM. Distribution of estrogen receptor beta containing cells in the brains of bacterial artificial chromosome transgenic mice. Brain research. 2010; 1351:74–96. [PubMed: 20599828]

Milner TA, Waters EM, Robinson DC, Pierce JP. Degenerating processes identified by electron microscopic immunocytochemical methods. Methods in molecular biology. 2011; 793:23–59. [PubMed: 21913092]

Miselis RR. The efferent projections of the subfornical organ of the rat: a circumventricular organ within a neural network subserving water balance. Brain research. 1981; 230(1–2):1–23. [PubMed: 7317773]

Mitterling KL, Spencer JL, Dziedzic N, Shenoy S, McCarthy K, Waters EM, McEwen BS, Milner TA. Cellular and subcellular localization of estrogen and progestin receptor immunoreactivities in the mouse hippocampus. The Journal of comparative neurology. 2010; 518(14):2729–2743. [PubMed: 20506473]

Morimoto K, Kurahashi Y, Shintani-Ishida K, Kawamura N, Miyashita M, Uji M, Tan N, Yoshida K. Estrogen replacement suppresses stress-induced cardiovascular responses in ovariectomized rats. American journal of physiology Heart and circulatory physiology. 2004; 287(5):H1950–1956. [PubMed: 15231501]

Mott NN, Pak TR. Estrogen signaling and the aging brain: context-dependent considerations for postmenopausal hormone therapy. ISRN endocrinology. 2013; 2013:814690. [PubMed: 23936665]

Nakamichi N, Yoneda Y. Functional proteins involved in regulation of intracellular Ca(2+) for drug development: desensitization of N-methyl-D-aspartate receptor channels. Journal of pharmacological sciences. 2005; 97(3):348–350. [PubMed: 15764843]

Nelson JF, Karelus K, Bergman MD, Felicio LS. Neuroendocrine involvement in aging: evidence from studies of reproductive aging and caloric restriction. Neurobiology of aging. 1995; 16(5):837–843. discussion 855–836. [PubMed: 8532119]

Nicholson DA, Trana R, Katz Y, Kath WL, Spruston N, Geinisman Y. Distance-dependent differences in synapse number and AMPA receptor expression in hippocampal CA1 pyramidal neurons. Neuron. 2006; 50(3):431–442. [PubMed: 16675397]

Nong Y, Huang YQ, Ju W, Kalia LV, Ahmadian G, Wang YT, Salter MW. Glycine binding primes NMDA receptor internalization. Nature. 2003; 422(6929):302–307. [PubMed: 12646920]

Nunn N, Womack M, Dart C, Barrett-Jolley R. Function and pharmacology of spinally-projecting sympathetic pre-autonomic neurones in the paraventricular nucleus of the hypothalamus. Current neuropharmacology. 2011; 9(2):262–277. [PubMed: 22131936]

Perello M, Raingo J. Leptin activates oxytocin neurons of the hypothalamic paraventricular nucleus in both control and diet-induced obese rodents. PloS one. 2013; 8(3):e59625. [PubMed: 23527232]

Peters, A.; Palay, S.; Webster, H. The fine structure of the nervous system. New York: Oxford UP; 1991.

Pierce JP, Kurucz OS, Milner TA. Morphometry of a peptidergic transmitter system: dynorphin B-like immunoreactivity in the rat hippocampal mossy fiber pathway before and after seizures. Hippocampus. 1999; 9(3):255–276. [PubMed: 10401641]

Polgar E, Thomson S, Maxwell DJ, Al-Khater K, Todd AJ. A population of large neurons in laminae III and IV of the rat spinal cord that have long dorsal dendrites and lack the neurokinin 1 receptor. The European journal of neuroscience. 2007; 26(6):1587–1598. [PubMed: 17880393]

Remondes M, Schuman EM. Direct cortical input modulates plasticity and spiking in CA1 pyramidal neurons. Nature. 2002; 416(6882):736–740. [PubMed: 11961555]

Shughrue PJ, Merchenthaler I. Distribution of estrogen receptor beta immunoreactivity in the rat central nervous system. The Journal of comparative neurology. 2001; 436(1):64–81. [PubMed: 11413547]

Siegel SJ, Brose N, Janssen WG, Gasic GP, Jahn R, Heinemann SF, Morrison JH. Regional, cellular, and ultrastructural distribution of N-methyl-D-aspartate receptor subunit 1 in monkey hippocampus. Proceedings of the National Academy of Sciences of the United States of America. 1994; 91(2):564–568. [PubMed: 8290563]

Siegel SJ, Janssen WG, Tullai JW, Rogers SW, Moran T, Heinemann SF, Morrison JH. Distribution of the excitatory amino acid receptor subunits GluR2(4) in monkey hippocampus and colocalization with subunits GluR5-7 and NMDAR1. J Neurosci. 1995; 15(4):2707–2719. [PubMed: 7722624]

Szymczak S, Kalita K, Jaworski J, Mioduszewska B, Savonenko A, Markowska A, Merchenthaler I, Kaczmarek L. Increased estrogen receptor beta expression correlates with decreased spine formation in the rat hippocampus. Hippocampus. 2006; 16(5):453–463. [PubMed: 16526034]

Tiwari S, Li L, Riazi S, Halagappa VK, Ecelbarger CM. Sex and age result in differential regulation of the renal thiazide-sensitive NaCl cotransporter and the epithelial sodium channel in angiotensin II-infused mice. American journal of nephrology. 2009; 30(6):554–562. [PubMed: 19844087]

Turner, CD.; Bagnara, JT. General Endocrinology. Philadelphia: W. B. Saunders; 1971.

Ueyama T, Tanioku T, Nuta J, Kujira K, Ito T, Nakai S, Tsuruo Y. Estrogen alters c-Fos response to immobilization stress in the brain of ovariectomized rats. Brain research. 2006; 1084(1):67–79. [PubMed: 16545785]

Volkmann K, Chen YY, Harris MP, Wullimann MF, Koster RW. The zebrafish cerebellar upper rhombic lip generates tegmental hindbrain nuclei by long-distance migration in an evolutionary conserved manner. The Journal of comparative neurology. 2010; 518(14):2794–2817. [PubMed: 20506476]

Wang G, Coleman CG, Chan J, Faraco G, Marques-Lopes J, Milner TA, Guruju MR, Anrather J, Davisson RL, Iadecola C, Pickel VM. Angiotensin-II slow-pressor hypertension enhances NMDA currents and Nox2-dependent superoxide production in hypothalamic paraventricular neurons. American journal of physiology Regulatory, integrative and comparative physiology. 2013

Wenthold RJ, Prybylowski K, Standley S, Sans N, Petralia RS. Trafficking of NMDA receptors. Annual review of pharmacology and toxicology. 2003; 43:335–358.

Wiinberg N, Hoegholm A, Christensen HR, Bang LE, Mikkelsen KL, Nielsen PE, Svendsen TL, Kampmann JP, Madsen NH, Bentzon MW. 24-h ambulatory blood pressure in 352 normal Danish subjects, related to age and gender. American journal of hypertension. 1995; 8(10 Pt 1):978–986. [PubMed: 8845079]

Xue B, Johnson AK, Hay M. Sex differences in angiotensin II- induced hypertension. Brazilian journal of medical and biological research = Revista brasileira de pesquisas medicas e biologicas / Sociedade Brasileira de Biofisica [et al]. 2007a; 40(5):727–734.

Xue B, Johnson AK, Hay M. Sex differences in angiotensin II- and aldosterone-induced hypertension: the central protective effects of estrogen. American journal of physiology Regulatory, integrative and comparative physiology. 2013

Xue B, Pamidimukkala J, Hay M. Sex differences in the development of angiotensin II-induced hypertension in conscious mice. American journal of physiology Heart and circulatory physiology. 2005; 288(5):H2177–2184. [PubMed: 15626687]

Xue B, Pamidimukkala J, Lubahn DB, Hay M. Estrogen receptor-alpha mediates estrogen protection from angiotensin II-induced hypertension in conscious female mice. American journal of physiology Heart and circulatory physiology. 2007b; 292(4):H1770–1776. [PubMed: 17142339]

Xue B, Singh M, Guo F, Hay M, Johnson AK. Protective actions of estrogen on angiotensin II-induced hypertension: role of central nitric oxide. American journal of physiology Heart and circulatory physiology. 2009; 297(5):H1638–1646. [PubMed: 19734362]

Xue B, Zhao Y, Johnson AK, Hay M. Central estrogen inhibition of angiotensin II-induced hypertension in male mice and the role of reactive oxygen species. American journal of physiology Heart and circulatory physiology. 2008; 295(3):H1025–H1032. [PubMed: 18599599]

Ye ZY, Li L, Li DP, Pan HL. Casein kinase 2-mediated synaptic GluN2A up-regulation increases N-methyl-D-aspartate receptor activity and excitability of hypothalamic neurons in hypertension. The Journal of biological chemistry. 2012; 287(21):17438–17446. [PubMed: 22474321]

Zheng H, Liu X, Li Y, Sharma NM, Patel KP. Gene transfer of neuronal nitric oxide synthase to the paraventricular nucleus reduces the enhanced glutamatergic tone in rats with chronic heart failure. Hypertension. 2011; 58(5):966–973. [PubMed: 21968757]

Zuloaga DG, Zuloaga KL, Hinds LR, Carbone DL, Handa RJ. Estrogen receptor beta expression in the mouse forebrain: Age and sex differences. The Journal of comparative neurology. 2013

Zuo Z, Mahesh VB, Zamorano PL, Brann DW. Decreased gonadotropin-releasing hormone neurosecretory response to glutamate agonists in middle-aged female rats on proestrus afternoon: a possible role in reproductive aging? Endocrinology. 1996; 137(6):2334–2338. [PubMed: 8641183]

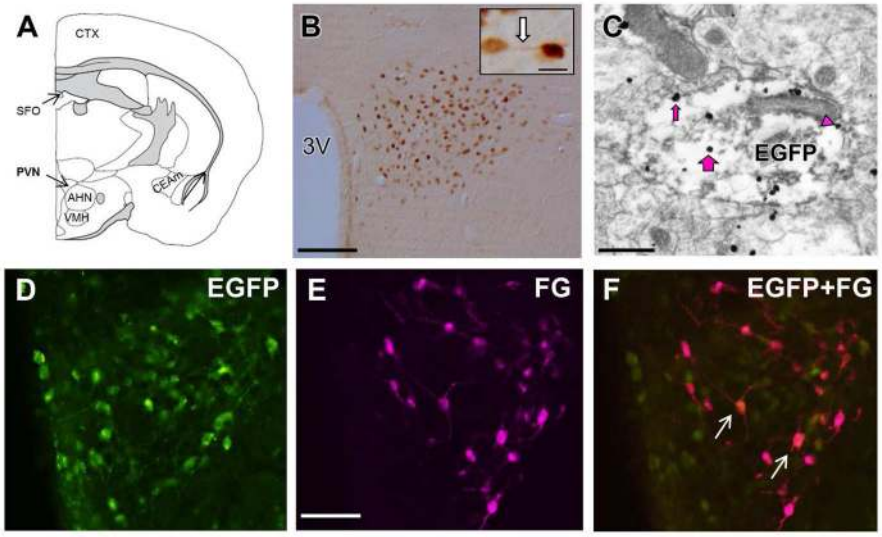

Figure 1. Estrogen receptor β (ERβ)-enhanced green fluorescent protein (EGFP)-labeled cells in the hypothalamic paraventricular nucleus (PVN)

A: Diagram of a coronal section of the mouse brain, showing a representative rostrocaudal level of the PVN containing ERβ-EGFP [modified from Hof et al. (2000)]. B: Numerous ERβ-EGFP-containing cells were found in the PVN. Higher magnification (inset) showed that dendritic processes (arrow) of PVN neurons can be identified. C: Representative immunoelectron microscopic picture showing NR1-silver-intensified immunogld (SIG) particles in an ERβ-EGFP-labeled (immunoperoxidase) PVN dendrite. Immunoperoxidase labeling for ERβ-EGFP (black arrow) was found throughout the cytoplasm of dendritic profiles. NR1-SIG particles (black dots) were localized in the plasmalemma (thin magenta arrow), near the plasmalemma (magenta arrowhead), and in the cytoplasm (thick magenta arrow). D–F: Spinally projecting ERβ-EGFP-labeled PVN neurons; D: ERβ-EGFP PVN neurons (green) labeled with anti-GFP antiserum; E: PVN neurons labeled with anti-Fluorogold (FG) antiserum (magenta); F: merge of D and E showed co-localization of GFP and FG (arrows). 3V, third ventricle; AHN, anterior hypothalamic nucleus; CEAm, central nucleus of the amygdala, medial part; CTX, cortex; SFO, subfornical organ; VMH, ventromedial nucleus of the hypothalamus. Scale bars: B, D–F = 0.5 mm; C, 500 nm; Inset, 25 μm.

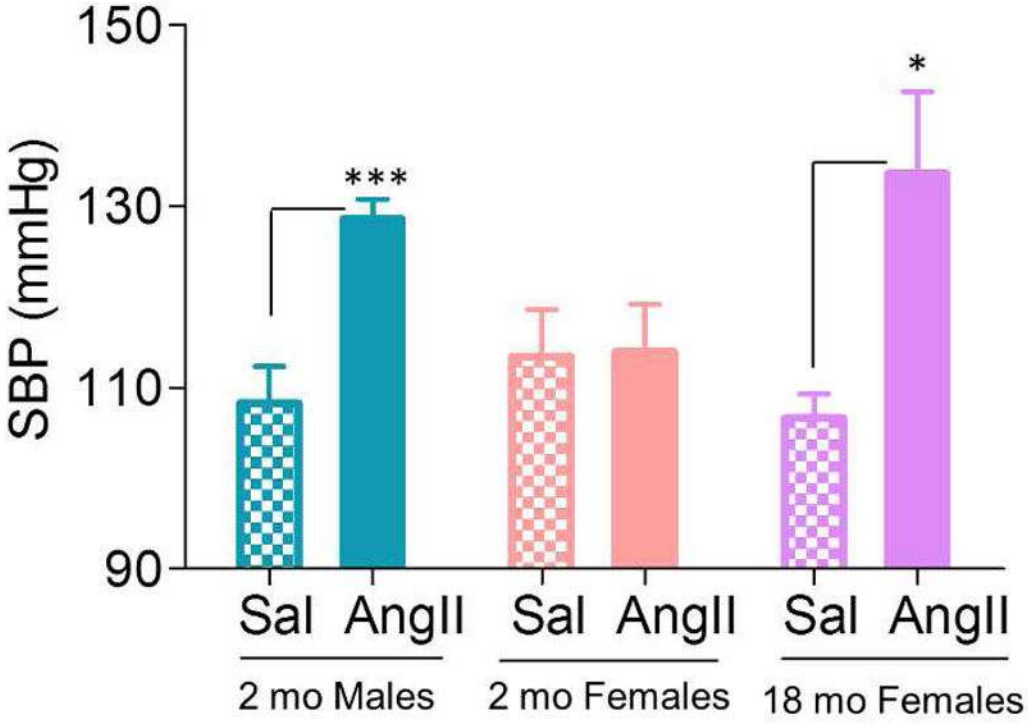

Figure 2. Angiotensin II (AngII) increases systolic blood pressure (SBP) in males and aged females but not in young females

AngII infusion induced significant SBP increases in males (blue, $p < 0.001$) and aged females (purple, $p < 0.05$), but not in young females (pink). Sal, saline. *: $p < 0.05$, ***; $p < 0.001$

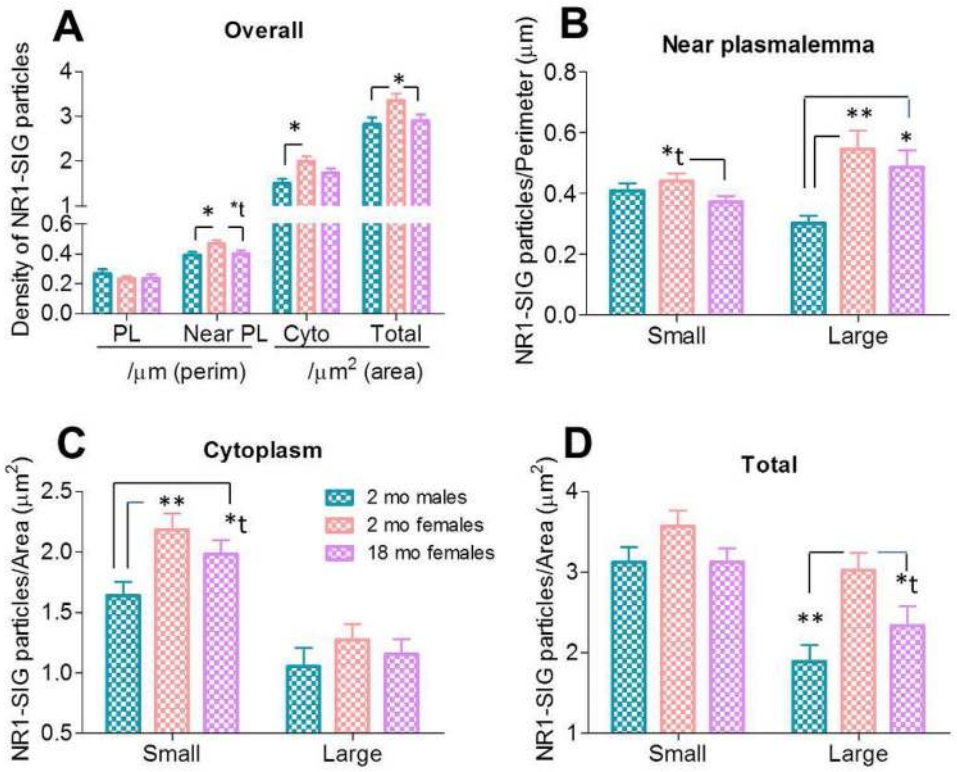

Figure 3. Baseline NR1 density in ERβ-EGFP-labeled PVN dendrites decreases with aging and is greater in young females than in age-matched males

A: In ERβ-EGFP dendrites, young females showed greater near-plasmalemmal ($p < 0.05$) and total ($p < 0.05$) NR1-SIG density than males and aged females, and greater cytoplasmic ($p < 0.05$) NR1-SIG density than males. B: In small ERβ-EGFP dendrites (< 1.0 um in diameter), young females showed greater near-plasmalemmal ($p < 0.05$) NR1-SIG density than aged females, whereas in large ERβ-EGFP dendrites (> 1.0 um in diameter), young and aged females showed greater near-plasmalemmal ($p < 0.05$) NR1-SIG density than males. C: In small ERβ-EGFP-containing dendrites, young and aged females showed greater cytoplasmic ($p < 0.05$) NR1-SIG density than males. No difference was observed in cytoplasmic NR1-SIG density in large ERβ-EGFP-labeled dendrites. D: In large ERβ-EGFP-containing dendrites, young females showed greater total ($p < 0.01$) NR1-SIG density than males and aged females. No difference was observed in total NR1-SIG density in small ERβ-EGFP dendrites. Perim, perimeter; PL, plasmalemma. *: $p < 0.05$, **: $p < 0.01$

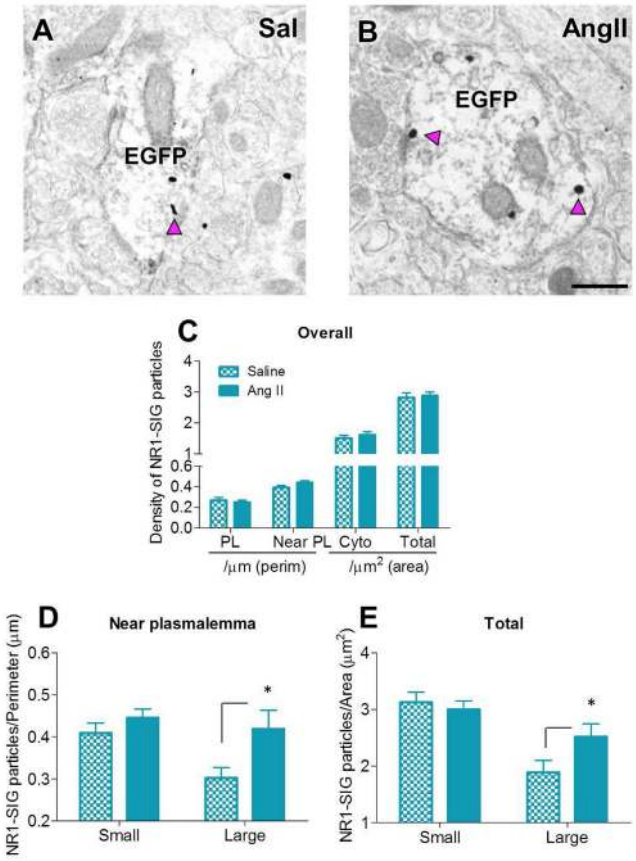

Figure 4. In males, AngII infusion increases near plasmalemmal and total NR1 density in large ERβ-EGFP-labeled PVN dendrites

A–B: Representative electron micrographs of large ERβ-EGFP-containing dendrites from saline- (**A**) and AngII-infused (**B**) males showing increased near plasmalemmal and total NR1-SIG density after AngII administration. Scale Bar = 500 nm. **C:** No differences were observed in overall NR1-SIG subcellular distribution in ERβ-EGFP dendrites. **D, E:** In large ERβ-EGFP dendrites, AngII infusion significantly increased near plasmalemmal ($p < 0.05$, **D**) and total ($p < 0.05$, **E**) NR1-SIG density comparing to saline infusion. No difference was observed in small ERβ-EGFP dendrites. *: $p < 0.05$

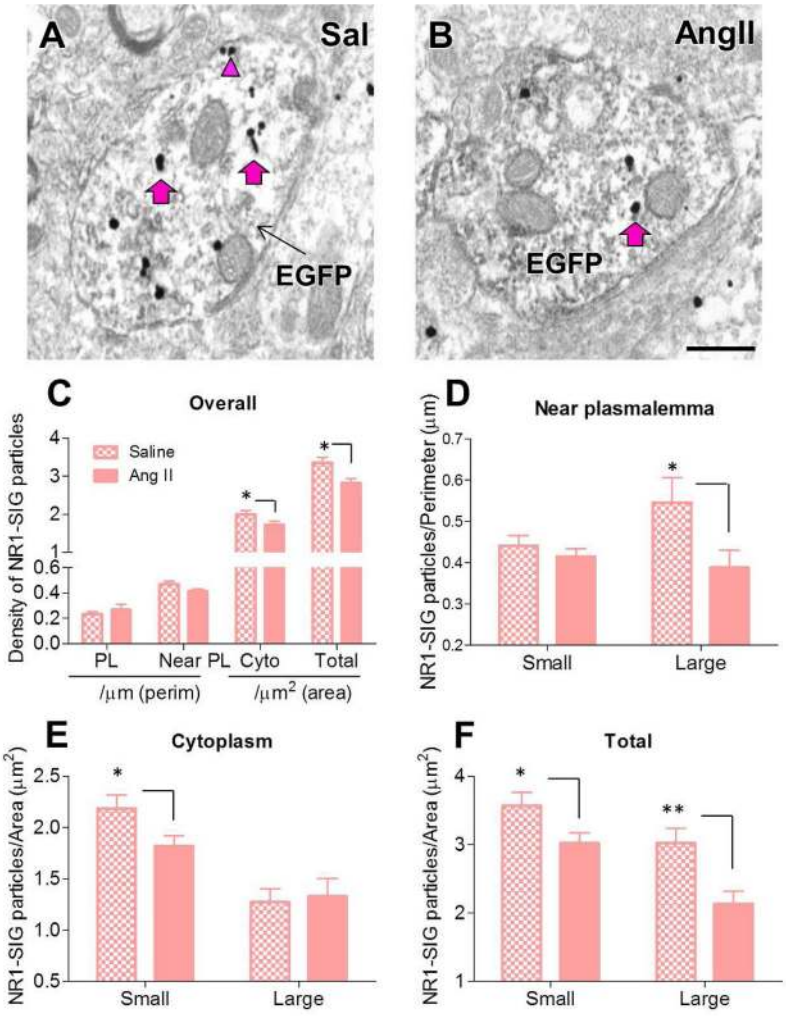

Figure 5. In young females, AngII infusion significantly decreased NR1 density in ERβ-EGFP-labeled PVN dendrites

A–B: Representative electron micrographs of ERβ-EGFP-containing dendrites from saline-(**A**) and AngII-infused (**B**) young females showing decreased near plasmalemmal, cytoplasmic and total NR1-SIG density after AngII administration. Scale bar = 500 nm. **C:** AngII infusion significantly decreased cytoplasmic ($p < 0.05$) and total ($p < 0.05$) NR1-SIG density in ERβ-EGFP dendrites. **D:** In small ERβ-EGFP dendrites, AngII-administered animals showed decreased near plasmalemmal NR1-SIG density ($p < 0.05$). No difference was observed in near plasmalemmal NR1-SIG density in small ERβ-EGFP dendrites. **E:** In large ERβ-EGFP dendrites, AngII-infused animals showed decreased cytoplasmic ($p < 0.05$) NR1-SIG density. No difference was observed in cytoplasmic NR1-SIG density in small ERβ-EGFP dendrites. **F:** AngII infusion significantly decreased total ($p < 0.05$) NR1-SIG density in small and large ERβ-EGFP dendrites. *: $p < 0.05$, **: $p < 0.01$

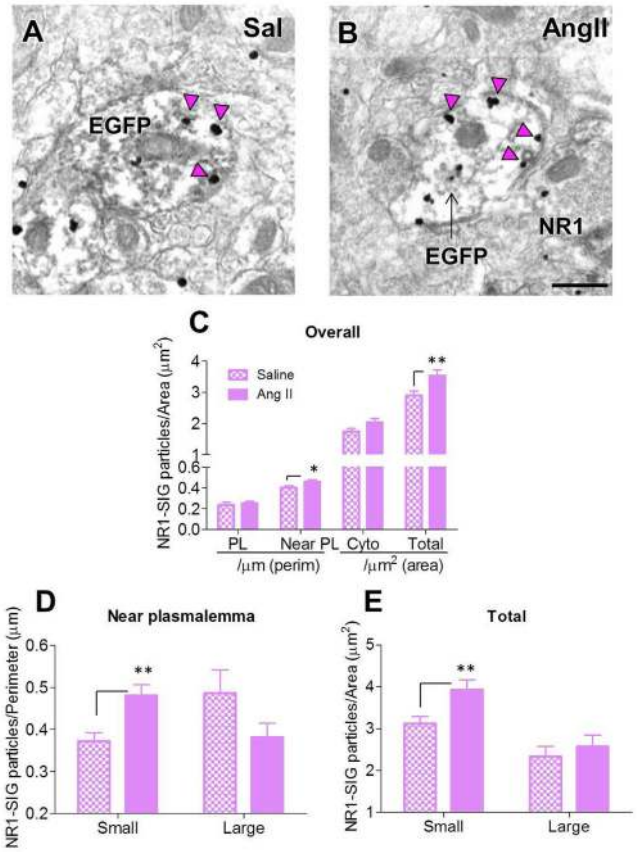

Figure 6. In aged females, AngII infusion significantly increased NR1 density in ERβ-EGFP-labeled PVN dendrites

A–B: Representative electron micrographs of ERβ-EGFP dendrites from saline- (**A**) and AngII-infused (**B**) aged females showing increased near plasmalemmal and total NR1-SIG density after AngII administration. Scale bar = 500 nm. **C:** AngII infusion significantly increased near plasmalemmal ($p < 0.05$) and total ($p < 0.01$) NR1-SIG density in ERβ-EGFP dendrites. **D, E:** In small ERβ-EGFP dendrites, AngII infusion elicited increased near plasmalemmal ($p < 0.05$, **D**) and total ($p < 0.05$, **E**) NR1-SIG density. No difference was observed in large ERβ-EGFP dendrites. *: $p < 0.05$, **: $p < 0.01$

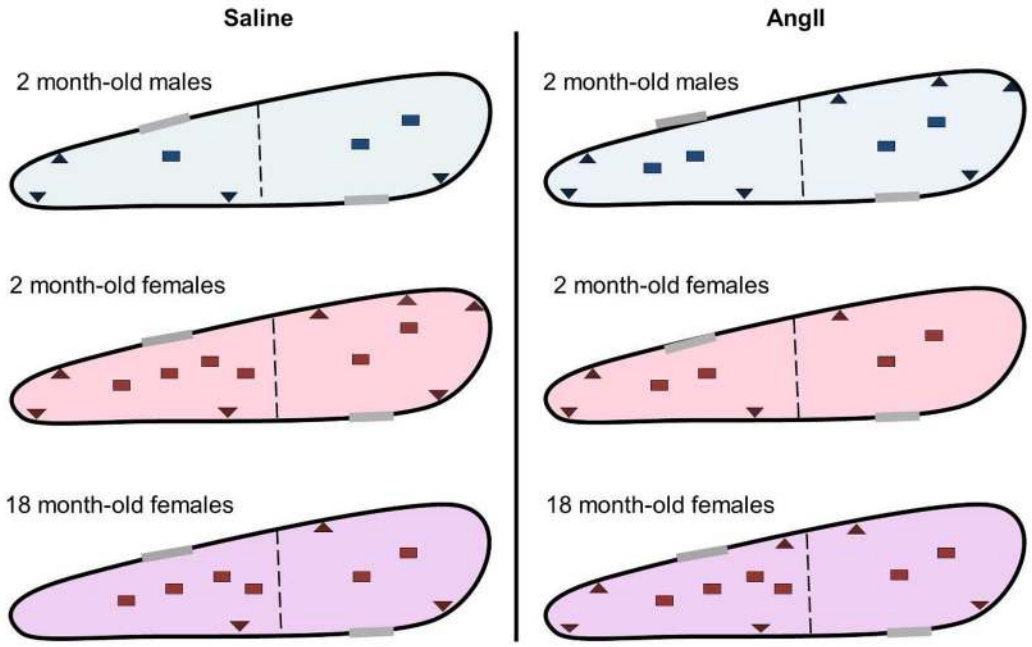

Figure 7. Schematic diagram summarizing the sex and age differences, and the AngII-induced effects on the density and trafficking of NR1 in ERβ-EGFP dendrites in the PVN

NR1-SIG particles are located near the plasmalemma (triangle) and in the cytoplasm (square) of ERβ-EGFP dendrites. No differences were observed in plasmalemmal NR1-SIG. Dashed line indicates division between small and large ERβ-EGFP dendrites and gray shadings on membranes indicate synapses. **Saline infusion**: Young female mice show greater near plasmalemmal, cytoplasmic and total NR1-SIG density than males, and greater near plasmalemmal and total NR1-SIG density than aged females. In small (distal) ERβ-EGFP dendrites, young females show greater cytoplasmic NR1-SIG density than males, and greater near plasmalemmal NR1-SIG density than aged females. Moreover, aged females show greater cytoplasmic NR- SIG density than males. In large (proximal) ERβ-EGFP dendrites, young and aged females show greater near plasmalemmal NR1-SIG density than males. Moreover, young females show greater total NR1-SIG density than males and aged females. **AngII infusion:** In males, AngII infusion increaseds near plasmalemmal and total NR1-SIG density in large PVN ERβ-EGFP dendrites in comparison with saline-infused controls. In young females, AngII infusion decreases cytoplasmic and total NR1-SIG density in ERβ-EGFP dendrites (both overall and small dendrites) in comparison with saline-infused controls. In large ERβ-EGFP dendrites, AngII infusion decreases near plasmalemmal and total NR1-SIG density. In aged females, AngII infusion increases near plasmalemmal and total NR1-SIG density in ERβ-EGFP dendrites (both overall and small dendrites).

Table 1

Antibodies used in study.

GFP	Chicken antibody against GFP – recombinant protein	Aves labs, GFP-1020, chicken, polyclonal
NMDAR1	Mouse antibody against NMDAR1 (aa. 660–811) – recombinant protein	BD Biosciences, 556308, mouse, monoclonal
FluGgp	Guinea pig antibody raised against FG (glutaraldehyde conjugate)	Protos Biotech Corp, NM-101, guinea pig